Plant, Cell & Environment

Plant, Cell and Environment (2016) **39**, 165–173 doi: 10.1111/pce.12603

Original Article

The chloroplastic DEVH-box RNA helicase INCREASED SIZE EXCLUSION LIMIT 2 involved in plasmodesmata regulation is required for group II intron splicing

Nicolas Carlotto[1], Sonia Wirth[1], Nicolas Furman[1], Nazarena Ferreyra Solari[2], Federico Ariel[3], Martin Crespi[3] & Ken Kobayashi[1]

[1]*Laboratorio de Agrobiotecnología, Instituto de Biodiversidad y Biología Experimental Aplicada (IBBEA-CONICET-UBA), Departamento de Fisiología, Biología Molecular y Celular, Facultad de Ciencias Exactas y Naturales, Universidad de Buenos Aires, Buenos Aires, Argentina,* [2]*Instituto de Investigación en Biomedicina de Buenos Aires (IBioBA) – CONICET – Partner Institute of the Max Planck Society, Buenos Aires, Argentina and* [3]*Institute of Plant Sciences Paris-Saclay (IPS2), UMR 9213/UMR1403, CNRS, INRA, Université Paris-Sud, Université d'Evry, Université Paris-Diderot, Sorbonne Paris-Cité, Bâtiment 630, 91405 Orsay, France*

ABSTRACT

***INCREASED SIZE EXCLUSION LIMIT 2* (*ISE2*) encodes a putative DEVH-box RNA helicase originally identified through a genetic screening for *Arabidopsis* mutants altered in plasmodesmata (PD) aperture. Depletion of ISE2 also affects chloroplasts activity, decreases accumulation of photosynthetic pigments and alters expression of photosynthetic genes. In this work, we show the chloroplast localization of ISE2 and decipher its role in plastidic RNA processing and, consequently, PD function. Group II intron-containing RNAs from chloroplasts exhibit defective splicing in *ise2* mutants and *ISE2*-silenced plants, compromising plastid viability. Furthermore, RNA immunoprecipitation suggests that ISE2 binds *in vivo* to several splicing-regulated RNAs. Finally, we show that the chloroplast *clpr2* mutant (defective in a subunit of a plastidic Clp protease) also exhibits abnormal PD function during embryogenesis, supporting the idea that chloroplast RNA processing is required to regulate cell–cell communication in plants.**

Key-words: chloroplast; Retrograde signals; cell-to-cell communication.

INTRODUCTION

Plasmodesmata (PD) are plant intercellular symplastic channels playing important roles for development, differentiation and organogenesis. The *INCREASED SIZE EXCLUSION LIMIT 2* gene (*ISE2*, AT1G70070) encodes a putative DEVH-box RNA helicase in *Arabidopsis thaliana*, and its mutation causes embryo-defective phenotype. The lack of *ISE2* prevents the down-regulation of the size exclusion limit (SEL) of PD during embryogenesis after the torpedo stage (Kim *et al.* 2002), and this was partially associated with the increment of branched and twinned PD (Kobayashi *et al.* 2007; Burch-Smith & Zambryski 2010). A genome-wide expression analysis of *ise2* mutant embryos revealed altered expression of many photosynthetic-related genes, in addition to cell wall-associated and PD-targeted proteins (Burch-Smith *et al.* 2011; Brunkard *et al.* 2013). Past studies have shown that ISE2 localizes to the chloroplast (Burch-Smith *et al.* 2011). In agreement, chloroplast proteome (The Plant Proteome Data Base) indicates that ISE2 is found in organelles (Zybailov *et al.* 2008), although its function in the chloroplast remains unknown.

Plastid maturation takes place during embryogenesis, together with accumulation of photosynthetic pigments and essential metabolites such as vitamins, hormones and lipids. In adult plants, the retrograde signals from chloroplast to the nucleus modulate a wide range of physiological processes from stress responsiveness, alternative splicing, to circadian rhythm (Woodson & Chory 2008; Petrillo *et al.* 2014).

Chloroplast RNAs are mostly regulated through splicing, editing and RNA decay pathways (Stern *et al.* 2010). Chloroplast-targeted nuclear encoded RNA binding proteins mainly include pentatricopeptides repeat (PPR) proteins and RNA helicases (Schmitz-Linneweber & Small 2008; Kroeger *et al.* 2009; Ruwe *et al.* 2011; Majeran *et al.* 2012), several of which have been previously characterized to be involved in RNA metabolism (de Longevialle *et al.* 2008; Melonek *et al.* 2010; Asakura *et al.* 2012; Chi *et al.* 2012).

In *Arabidopsis*, a total of 58 RNA helicases contain a DEAD-box domain (Aubourg *et al.* 1999; Mingam *et al.* 2004), seven of which (named RH3, RH22, RH26, RH39, RH47, RH50 and RH58) are localized in chloroplasts (Zybailov *et al.* 2008; Olinares *et al.* 2010). RH3 was detected in nucleoid-enriched fraction of chloroplasts and is involved in the splicing of group II intron and maturation of 50S subunit of plastid ribosomes (Asakura *et al.* 2012; Lee *et al.* 2012). RH22 and RH39 seem to be required for the proper maturation of plastid ribosomal RNAs (Nishimura *et al.* 2010; Chi *et al.* 2012). Besides ISE2, two other DEVH-box RNA helicases were reported previously in *Arabidopsis*: the nucleolocated MTR4 (AT1G59760), required for proper nuclear rRNA biogenesis, and AtHELPS (AT3G46960), involved in the potassium-deprivation stress response (Lange *et al.* 2011; Xu *et al.* 2011; Lange *et al.* 2014).

Correspondence: K. Kobayashi. e-mail: ken@fbmc.fcen.uba.ar

As ISE2 encodes the sole DEVH-box RNA helicase found to be targeted into chloroplasts, we investigated the role of ISE2 during organelle RNA maturation. Here, we demonstrate that ISE2 depletion causes splicing defects of chloroplasts transcripts containing group II introns. Furthermore, we show that ISE2 directly binds to chloroplast RNA targets *in vivo*. Strikingly, we discovered that a Clp protease mutant impaired in chloroplast splicing shows a similar increased PD aperture phenotype during the embryogenesis. Hence, regulation of splicing in chloroplasts impacts the regulation of intercellular communication through PD channels.

MATERIALS AND METHODS

Plant materials and growth conditions

Transgenic *35S*: *ISE2*:*GFP* (*ISE2*:*GFP*) and mutant *ise2-2* (*ise2*) plants and seedlings were handled as previously described (Kim *et al.* 2002; Kobayashi *et al.* 2007). *clpr2* (Salk_016774) was obtained from the *Arabidopsis* Biological Resource Center, and homozygous mutant embryos obtained from heterozygous plants were directly used in this study. Plants were grown in 16-h light/8-h dark under white fluorescent light at 22 °C.

RNA extraction and Northern blot

RNAs were extracted from the *Arabidopsis* seedlings using RNAzol® RT reagent (Molecular Research Center, Cincinnati, OH, USA) according to the manufacturer's instructions. Of total RNA of each sample, 3 μg were fractionated in denaturing 3-(N-Morpholino) propanesulfonic acid (MOPS)-formaldehyde gels (agarose 1%) and transferred to Hybond N+ Nylon membranes (Amersham, Piscataway, NJ, USA) by capillary blotting in SSC 10X and cross linked by UV (UV Stratalinker 2400; Stratagene, La Jolla, CA, USA). DNA probes were labelled with ^{32}P-CTP using PCR or random priming. Pre-hybridization and hybridization were carried out at 65 °C in Church's hybridization solution (Church & Gilbert 1984). After hybridization, probed membranes were washed with 2X Saline Sodium Citrate buffer PH7 (SSC), 0.1% sodium dodecyl sulphate (SDS) for 15 min at room temperature, after that at hybridization temperature with the same solution for 15 min, then with 0.2X SSC, 0.1% SDS for 15 min and finally washed with 0.1X SSC, 0.1% SDS for 15 min. Membranes were exposed to X-ray film (Kodak, Rochester, NY, USA).

cDNA synthesis

RNA extracted from *Arabidopsis* seedlings was treated with RNase-free DNase I (New England Biolabs, Inc., Beverly, MA, USA) for cDNA synthesis using the ImProm-II™ Reverse Transcriptase (Promega, Madison, WI, USA) with oligo dT, random hexamer primers or gene-specific primers (for chloroplast genes). Reactions containing all the reagents except reverse transcriptase were used as a negative control of PCR.

Western blot

Total protein extract from fresh leaves was prepared as previously described (Kobayashi *et al.* 2007). Quantified proteins were analysed in SDS–polyacrylamide gel electrophoresis (PAGE) and transferred to nitrocellulose membrane (Amersham™Hybond ECL). Primary antibodies against GFP (ab290; Abcam Ltd Cambridge, UK) and ribulose 1·5-bisphosphate carboxylase/oxygenase (polyclonal rabbit anti-RbcL antibody Agrisera AS03037) were employed according to provider instructions and goat anti-rabbit IgG-Horseradish peroxidase (HRP) (Santa Cruz Biotechnologies SC 2004, Santa Cruz, CA, USA) was employed as secondary antibody. Membranes were incubated accordingly to standard protocol and revealed using Enhanced chemiluminescence (ECL) system (Pierce, Rockford, IL, USA).

Chloroplasts isolation

Chloroplasts were purified by sucrose density gradient centrifugation from 5 g of leaf tissue according to Nishimura *et al.* (1976). Intact chloroplast fraction precipitated at 3800 g, 4 °C for 10 min, and pellet was resuspended in 2 ml of BH10 buffer (Tris-HCl 30 mM pH 7.4, $MgCl_2$ 5 mM and sucrose 10%) supplemented with proteases inhibitor (E complete mini; Roche, Indianapolis, IN, USA). The images were acquired using confocal microscopy Zeiss AxioObserverZ1-LSM710 and processed using ZEN 2011 Black edition.

RNA immunoprecipitation assay

For chloroplasts lyses, pellet was frozen three times during 30 s in liquid N_2, resuspended in 3 ml of CoIP buffer (Tris-HCl 20 mM pH 8, $MgCl_2$ 2 mM, NP40 0.5%, ethylenediaminetetraacetic acid (EDTA) 1 mM, NaCl 150 mM, glycerol 10%, DTT 1 mM, KCl 50 mM, RNAseOUT 100 U in 5 ml buffer, and protease inhibitor) and passed through a 21 gauge needle several times. Lysate was divided into three 1.5 ml tubes and centrifuged for 10 min 11000 g at 4 °C. Supernatant (input) was further used for the immunoprecipitation performed by Direct ChIP Protocol of the Diagenode IP-Star SX-86 Compact robot, using 50 μl of Dynabeads® – Protein A (Novex 10008D; Life Technologies, Rockville, MD, USA), anti-IgG (Millipore, Billerica, MA, USA) or anti-GFP (632381; Clontech, Mountain View, CA, USA) antibodies. Beads were washed three times for 5 min at 4 °C with Wash Buffer 1 (NaCl 150 mM, Triton 1%, NP-40 0.5%, EDTA 1 mM, Tris-HCl 20 mM pH 7.5) and once with Wash Buffer 2 (Tris-HCl 20 mM pH 8) instead of the CoIP buffers, and finally resuspended in 100 μl Proteinase K buffer (Tris-HCl 100 mM pH7.4, NaCl 50 mM, EDTA 10 mM). After Proteinase K (AM2546; Ambion, Austin, TX, USA) treatment, beads were removed with a magneto, and the supernatants were transferred to a 2 ml tube. RNA was extracted from 200–600 μl of supernatant with 1 ml of TriReagent® (Sigma-Aldrich T9424, St Louis, MO, USA) as indicated by the manufacturer.

Plastid transcript splicing analysis by RT-PCR

Splicing analysis was performed as described by Babiychuk *et al.* (2011). Probes used for RT and PCR are listed in Supporting Information Table S1.

qRT-PCR

SYBR® Green PCR Master Mix (Applied Biosystems, ABI, Foster City, CA, USA) was used for PCR mixes. All reactions were run in triplicate for each sample at CFX96 Touch Real-Time PCR Detection system (Bio-Rad, Hercules, CA, USA). The primers used are listed in Supporting Information Table S1. Values were relativized to that for U-box domain-containing protein (Ubiquitin, AT5G15400) or actin2 (AT3G18780). Averages of three independent reactions ± standard deviations (s.d) were determined. The relative expression level was calculated using the $2^{-\Delta CT}$ and fold determined by using $2^{-\Delta\Delta CT}$ method (Schmittgen & Livak 2008).

Dye-loading assay

Dye-loading was performed as previously described (Kim *et al.* 2002; Kobayashi *et al.* 2007). The experiments were repeated three times, and positive or negative loading embryos were scored individually by analysing microscope images.

RESULTS

Overexpression of ISE2–GFP leads to spontaneous silencing and a chlorotic phenotype

For the study of ISE2 function, we used a stable transgenic line (*ISE2-GFP*) constitutively expressing an ISE2-GFP *(green fluorescent protein)* fusion protein in an *ise2-2* homozygous mutant background that fully rescued the phenotype (Kobayashi *et al.* 2007). Although *ISE2-GFP* plants grow normally and are phenotypically indistinguishable from Col-0 [wild-type (WT)] plants, we observed 3 to 5% of T3 plants showing chlorotic leaves with serrated margins (named *ise2-gfp*, Fig. 1a). This chlorosis could be detected at any stage, but often begun at an early age (usually from four to six true leaves stage), and spread from the base of fully expanded leaves to other parts of the plant, including the inflorescence shoots. The steady-state level of ISE2 mRNAs in chlorotic leaves was significantly lower compared with green leaves (Fig. 1b). Therefore, we assumed that the chlorosis would phenocopy *ise2* mutant due to the fact that the remnant level of *ISE2-GFP* transcripts detected in chlorotic leaves were insufficient to rescue the mutant phenotype. Supporting these observations, GFP fluorescence was not detectable by confocal microscopy and ISE2-GFP protein level was strongly reduced in chlorotic leaves (Supporting Information Fig. S1a).

As there were previous evidences of ISE2's chloroplast localization (Burch-Smith *et al.* 2011), we analysed protein extracts from purified chloroplasts to confirm the ISE2-GFP subcellular localization in *ISE2-GFP* green plants. A specific

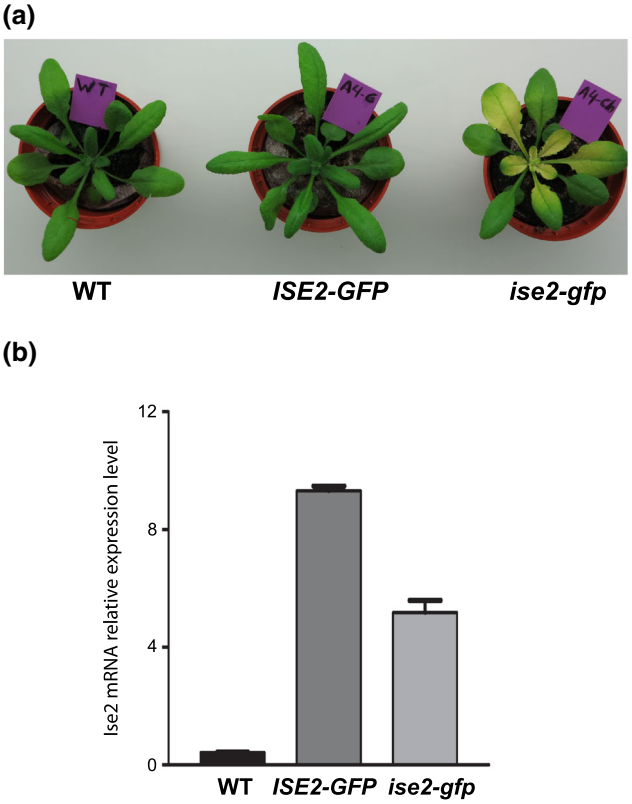

Figure 1. (a) Characterization of transgenic *ISE2-GFP* line. Phenotype of Col-0 (WT), ISE2-GFP green plant (*ISE2-GFP*) and chlorotic plant (*ise2-gfp*). *ISE2-GFP* plants were indistinguishable from WT plants. (b) Real-time qRT-PCR of Ise2 mRNAs. Relative expression levels of Ise2 mRNA are expressed. Error bars correspond to the standard deviation from triplicate determinations. Analysis of variance test followed by Bonferroni's multiple comparison test were performed. p-value < 0.001.

band of approximately MW 160 kDa was detected in the plastidic fractions revealed by Western blot (Supporting Information Fig. S1b). In agreement with previous published time-lapse confocal microscopy images from *Nicotiana benthamiana* leaves expressing ISE2-GFP, we observed ISE2-GFP discrete foci within isolated chloroplasts from *ISE2-GFP* plants (Supporting Information Fig. S1c).

ISE 2 is required for group II intron splicing in chloroplasts

Because ISE2 encodes for a putative RNA helicase and is located in chloroplasts (Fig. S1c), we assessed whether knock-out (*ise2*) or knock-down (*ise2-gfp*) could be linked to alterations in plastidic RNA processing, as described for other plastidic RNA helicases and RNA binding proteins (Babiychuk *et al.* 2011; Asakura *et al.* 2012). To this end, we analysed splicing patterns for four chloroplast genes through the amplification of spliced and unspliced variants by RT-PCR.

For *ATP synthase subunit* (*atpF*) and *Ribosomal protein L2* (*rpl2*) mRNAs, two transcripts containing subtype IIa introns, we detected increased accumulation of unspliced

intermediaries both in *ise2* and *ise2-gfp* plants, compared with WT (Fig. 2a and b). We then analysed the splicing profile of the *Ribosomal protein S12* (*rps12*) mRNA, which requires the removal of a subtype IIb intron by trans-splicing in addition to a subtype IIa intron MatK-dependent splicing (Babiychuk *et al.* 2011). We observed that *rps12* trans-splicing occurs nearly normal in *ise2-gfp* and *ise2* mutants, although larger immature unprocessed transcripts bands were also detected, presumably due to subtype IIa intron retention (Fig. 2c). Finally, we analysed the *Caseinolytic protease PP1* (*clpP*) mRNA, which contains a subtype IIa intron independent of MatK and therefore independent of the organelle translation state (Babiychuk *et al.* 2011), in addition to a subtype IIb intron. Consistently, larger bands were detected in samples of *ise2-gfp* leaves and *ise2* plants, corresponding to the full-length unprocessed pre-mRNA, based on their estimated size of 1100 bp (Fig. 2d).

As shown in the gel image of Fig. 3, a marked reduction of the plastidic 16S and 23S rRNAs is observed in samples from *ise2* mutant seedlings (Fig. 3a). Similarly, the 23S seems also reduced in *ISE2* silenced (*ise2-gfp*) leaves compared with *ISE2-GFP* and WT leaves (Supporting Information Fig. S3) suggesting impaired posttranscriptional regulation of plastid gene expression. The alteration of the splicing pattern of *rpl2* was further confirmed by Northern blot. Two specific probes were used for the *rpl2*: one recognizes the exon1 containing sequence, whereas the other hybridizes the intronic sequence. In WT, bands comprising between 1.7 and 2 kb in estimated sizes were clearly detected with an exon specific probe, presumably corresponding to processed *rpl2* mRNAs (Hammani & Barkan 2014). Similar bands patterns were also observed in *ise2*. Remarkably, another chloroplast mutant *clpr2* exhibiting splicing defects (Asakura *et al.* 2012)

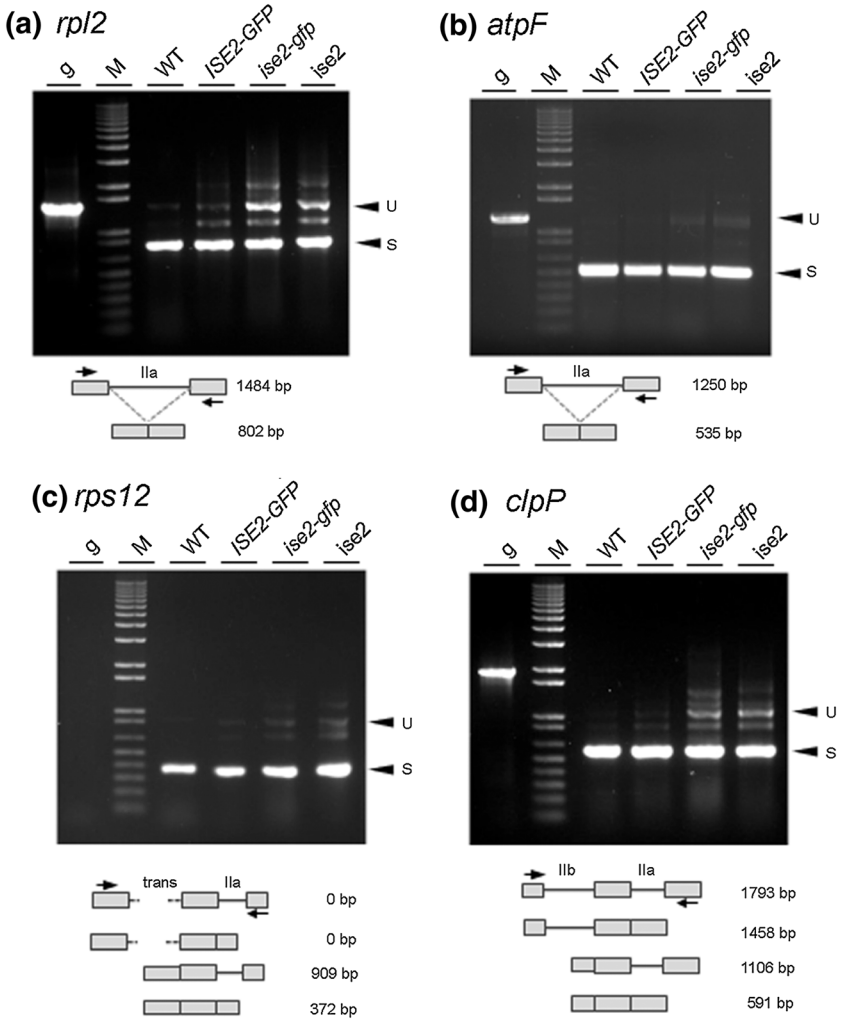

Figure 2. Analysis of plastid gene splicing in transgenic line and *ise2* mutant. WT, *ISE2-GFP*, *ise2-gfp* and *ise2* cDNAs for (a) *rpl2*, (b) *atpF*, (c) *rps12* or (d) *clpP* plastid genes were synthesized using gene-specific primers. The presence of fully spliced (s) and unspliced (u) intermediaries was analysed by PCR amplification, according to Babiychuk *et al.* (2011). Schematic drawing of intron–exon structure, intron group and predicted product sizes are indicated at the bottom of each panel. Arrows indicate position of specific primers used for PCR amplification (see also Supporting Information Fig. S3). The identity of *rpl2* larger band ('U') was confirmed by cloning and sequencing. g: full-length PCR product amplified using WT genomic DNA as template. M: 1 Kb plus DNA Ladder (Invitrogen Life Technologies, Carlsbad, CA, USA). Same PCR amplification pattern was observed for at least in two independent plants of each sample.

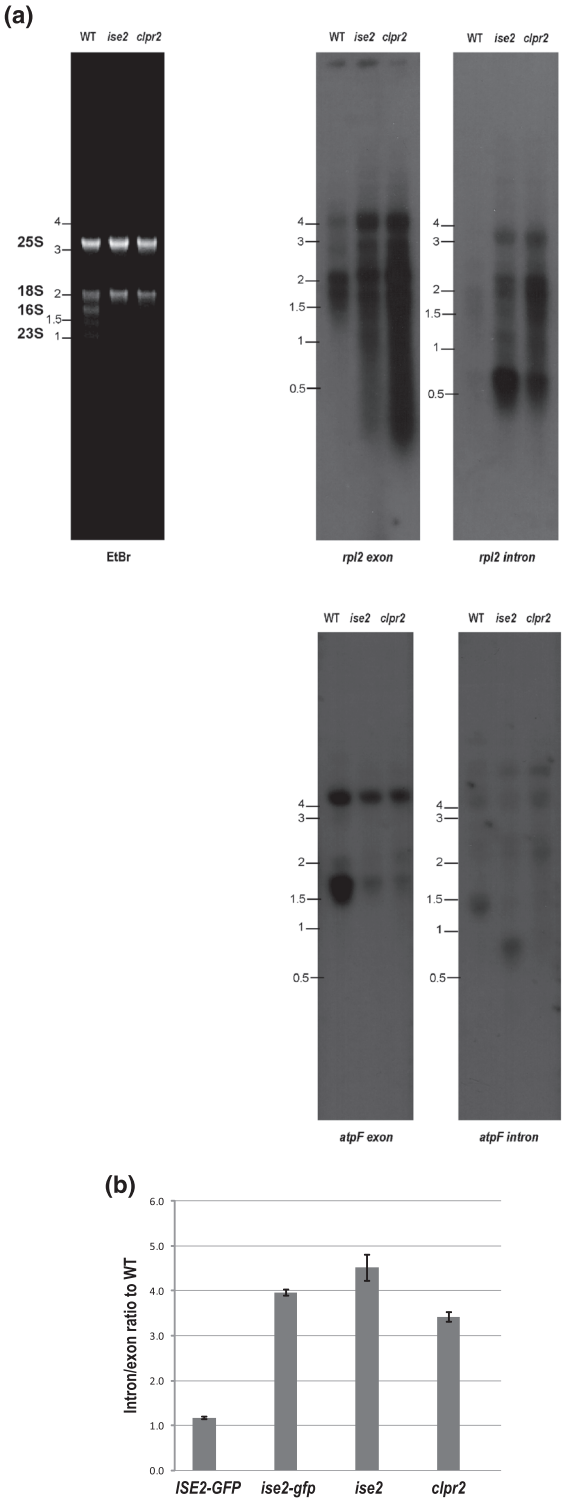

Figure 3. (a) Northern blot analysis. Total RNA (3 μg) of WT, *ise2* and *clpr2* mutant plants were analysed in denaturing agarose gels. Estimated sizes of bands are indicated. Probe identity is indicated for each blot. (b) Real-time qRT-PCR of *rpl2* mRNA. Relative expression levels of intron-containing and exon-containing mRNAs were compared quantitatively and expressed in fold with respect to WT. Error bar corresponds to the standard deviation from triplicate determinations. Except *ISE2-GFP*, all values were significantly higher than WT ($p < 0.01$) accordingly to a t-test

(see also Fig. 5a) also showed similar *rpl2* RNA pattern to *ise2*. Both mutants showed increased accumulation of higher bands ranging from 3 to 4 kb in their estimated sizes, probably corresponding to unprocessed transcripts. Supporting this, these bands were recognized by an intron specific probe (Fig. 3a). Importantly, hybridization with an intron specific probe gave a new clear band of approximately 2 kb in both mutant lanes, in addition to 1.3 to 1.5 kb bands, indicating enriched accumulation of intron-containing RNA species. Furthermore, a strong signal from a small band of approximate 0.75 kb was visible, as reported in maize chloroplast mutants (Hammani & Barkan 2014).

The blot probed with *atpF* exon specific sequence showed a band of approximately 1.5 kb in WT; this could correspond to the mature RNA. The same band was faint in both mutants (Fig. 3a). In contrast, a larger band of >4 kb in estimated size was visible in all lanes. When the blot was probed with intron-specific sequence, slightly enhanced >4 and 2.5 kb bands were observed in *clpr2* lane. A band of 0.75 kb was also enhanced in *ise2* lane.

In order to quantify the alteration of RNA splicing, we performed qRT-PCR assay to determine the ratio between intron-containing and exon-containing *rlp2* RNAs. As shown in Fig. 3b, the relative amounts of intron-containing mRNAs in *ise2* and *clpr2* were significantly higher than in WT. Our results indicate that ISE2 participates in the splicing of group II introns in chloroplasts.

ISE 2 interacts with its RNA targets *in vivo*

To further demonstrate the role of ISE2 during plastidic transcript splicing, we performed RNA immunoprecipitation assays (RIPs) using chloroplast extracts, in GFP-tagged ISE2 plants. After RIP with GFP antibodies, specific qRT-PCR was performed for *rpl2*, *atpF*, *rps12* and *clpP* RNAs, whose accurate processing is dependent on ISE2 (Figs 2 and 3). Strikingly, we detected significant enrichment of the four transcripts using anti-GFP antibodies compared with control IgG in *ISE2-GFP* chloroplasts, as well as using anti-GFP antibodies in chloroplasts from WT leaves (Fig. 4), indicating a direct interaction of the four target RNAs with ISE2-containing complexes. Altogether, our results suggest that ISE2 controls chloroplast splicing of group II introns by its direct interaction.

Defective splicing in chloroplasts is associated to altered aperture of the plasmodesmata during embryogenesis

Considering that the knock-out of ISE2 prevents the down-regulation of the SEL of PD during embryogenesis after the torpedo stage (Kim *et al.* 2002), we wondered whether this phenotype is due to inaccurate splicing in chloroplasts. Then, we aimed to characterize the *clpr2* mutant, whose defective embryo phenotype strikingly resembles the morphology to *ise2* (Kim *et al.* 2013), and both of them exhibit splicing defects in *rpl2*, *atpF* and *clpP* (Figs 3, 4 & 5A). We observed that *rps12* trans-splicing occurs nearly normal in *clpr2* mutants, although

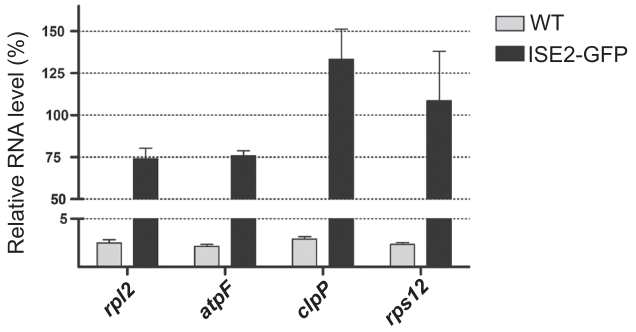

Figure 4. Quantification of bound RNAs upon immunoprecipitation (RIP). Transcripts for *rpl2*, *atpF*, *rps12 or clpP* were quantified by real-time RT-PCR from RIP obtained with anti-GFP or IgG antibody. The results were expressed as the relative between specific anti-GFP versus non-specific IgG-treated samples. All values were normalized to references RNA levels, from input and obtained by $2^{-\Delta Ct}$ method. For negative control corresponding to RNA not coprecipitated, we measured *rbcl* transcript without intron (not processed by ISE2), which gave an average ratio value of 18.08 ± 1.86 standard deviation from ISE2-GFP IP fraction using specific anti-GFP antibody. This value was significantly lower compared with those corresponding to four transcripts that we analysed. Two replicates were performed for each sample. Mean and standard deviation were calculated for each sample. ISE2-GFP values were significantly different to WT ($p < 0.01$) accordingly to a t-student.

larger immature unprocessed transcripts bands were also faintly detected, similarly to *ise2* (Fig. 2c). The gene Clpr2 (AT1G12410) encodes one of the subunits for Clp protease system needed for plastidic ribosome assembly, protein degradation, recycling and translation. Then, dye-loading assay was performed using *clpr2* torpedo embryos and *ise2* as positive control. Approximately 70% of *ise2* torpedo embryos showed loading of 10 kDa Dextran-Fluorescein isothiocyanate (FITC) (Fig. 5b, middle panel). As expected, the majority of the control WT or heterozygous torpedo embryos did not show apparent loading (Fig. 5b, top panel, less than 10% of total embryos tested were considered positives). Remarkably, 70% of *clpr2* torpedo embryos tested showed clear dye-loading phenotype (Fig. 5b, bottom panel), indicating that *clpr2* embryos have increased PD SELs; thus, it should be considered as an *increased size exclusion* limit (*ise*) mutant. Furthermore, *clpr2* constitutes another example of a chloroplast splicing defective mutant exhibiting an abnormal aperture of PD, supporting the cellular association between the two phenomena.

DISCUSSION

Significant advances in PD research were observed in the past few years, including the identification of its components, regulatory genes and a novel intracellular signalling mechanism ruling PD function (Maule *et al.* 2011; Burch-Smith & Zambryski 2012; Salmon & Bayer 2014). Nevertheless, the genetic and molecular mechanisms regulating PD architecture, number and functions during plant development remain to be deciphered.

Previous approaches to study PD functions included genetic screenings in *Arabidopsis* and identified the *ise2* and *ise1* mutants, the latter affecting a mitochondrial DEAD-box RNA helicase (Stonebloom *et al.* 2009) and *GFP arrested trafficking*

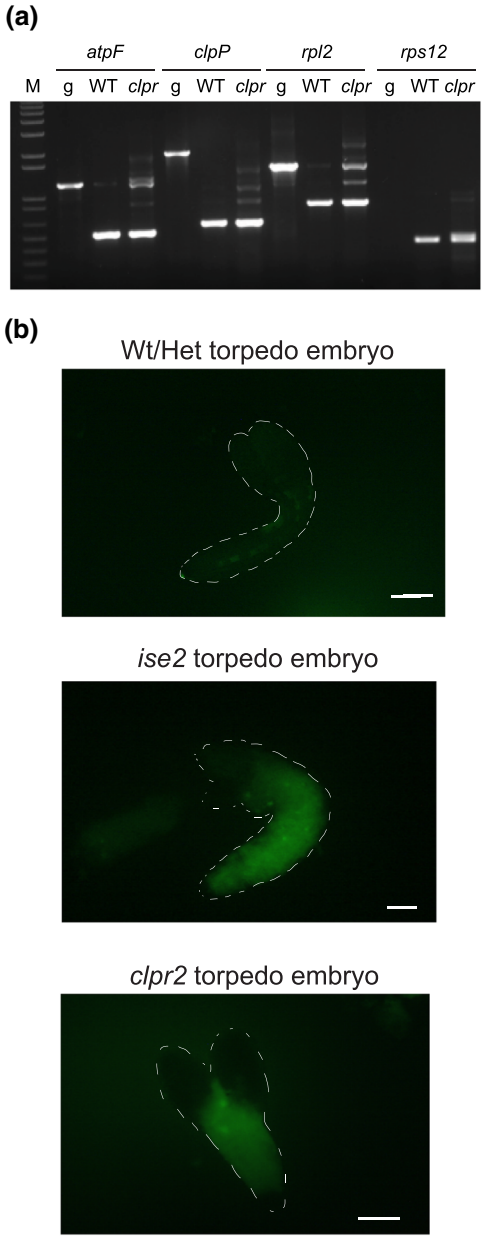

Figure 5. (a) Plastid gene splicing in *clpr2* mutants. cDNAs were synthesized using specific primers for *atpF*, *clpP*, *rpl2 or rps12*, and presence of fully spliced and unspliced intermediaries was analysed by PCR amplification, according to Babiychuk *et al.* (2011). g: full length PCR product amplified using WT genomic DNA as template. M: 1 Kb plus DNA Ladder (Invitrogen Life Technologies). (b) Dye-loading phenotype of mutant embryos. No clear dye-loading was observed with WT or heterozygous torpedo embryos (top panel) as was reported previously. Representative image of a positive 10 kDa Dextran-FITC loading of *ise2* torpedo embryo (middle panel) and *clpr2* embryo (bottom panel) with FITC signals within hypocotyls was observed in epifluorescence microscope. In total, 22 of *clpr2* and 25 of *ise2* homozygous torpedo embryos were included for analyses. Bar scale: 50 µm.

1 (*gat1*), which encodes a plastid Thioredoxin-m3 (TRX-m3) (Benitez-Alfonso *et al.* 2009). However, the *ise1* and *ise2* embryos have increased intercellular transport of 10 kDa Dextran-FITC after torpedo stage (Kim *et al.* 2002), in contrast

to *gat1* plants, which show reduced capacity to transport GFP through PD, due to increased callose accumulation at PD. Interestingly, all these mutants showed altered Reactive oxygen species (ROS) accumulation in their organelles (Stonebloom *et al*. 2012). Based on this finding, it was suggested that the redox status of organelles might indirectly regulate PD functions (Benitez-Alfonso *et al*. 2011; Burch-Smith & Zambryski 2012; Stonebloom *et al*. 2012), and an organelle-nucleus-PD signalling (ONPS) model was proposed to explain the regulation of PD function during embryogenesis by organelle-derived signals (Burch-Smith *et al*. 2011). These unknown signals probably belong to the retrograde signals that also regulate processes occurring in the nuclei (Nott *et al*. 2006). Although the true nature of these signals are still uncertain, several evidences point out that one of them may be chlorophyll precursors such as tetrapyrrole-derived compounds (Beale 2011).

In this work, we show that the ISE2-GFP is targeted into *Arabidopsis* chloroplasts, and it localizes probably at nucleoids. Because ISE2-GFP transgene could fully rescue the mutant phenotype (Kobayashi *et al*. 2007), we assumed that ISE2-GFP localization and function are *bona fide* equivalent to endogenous ISE2, and its silencing would mimic the mutant phenotype in adult plants. Recently, organelle proteome analysis served to identify ISE2-derived peptides within nucleoids fractions of *Arabidopsis* chloroplasts (Majeran *et al*. 2012). Similar organelle granular/foci to those of ISE2-GFP were observed for another DEAD-box RNA helicase, RH39, involved in the processing of 23S rRNA (Nishimura *et al*. 2010) as well as for the mitochondrial transcriptional termination factor/BELAYASMERT (mTERF/BSM) (Babiychuk *et al*. 2011).

We found that ISE2 controls the splicing of *rpl2*, *atpF* and *clpP* mRNAs. To further confirm the role of ISE2 in chloroplast splicing, RIP was used to determine direct interaction between ISE2 and its RNA targets.

A mutation with altered *atpF* splicing was previously reported to provoke chlorosis (Jenkins *et al*. 1997). Furthermore, the reduced level of *rpl2* affects ribosome assembly and translation in the organelle (Hess *et al*. 1994; Chi *et al*. 2012). Clp protease activity regulates factors involved in 23S rRNA-processing and organelle translation (Sjogren *et al*. 2006; Zheng *et al*. 2006; Olinares *et al*. 2010; Kim *et al*. 2013). Thus, ISE2 defects might additionally decrease translation in chloroplast because of Clp system deficiency, contributing to the chlorotic phenotype. Noteworthy, the translation impairment found in the *ise2* mutant and chlorotic leaves seems rather mild, (e.g. compared with antibiotic treatment; Babiychuk *et al*. 2011), because the trans-splicing of *rps12* in these leaves was not completely inhibited.

Here, we provide strong evidence that accurate splicing is required for normal chloroplast development and PD regulation, likely due to retrograde signals controlling the transcription of nuclear PD-related genes, which has been already proposed by ONPS model (Burch-Smith *et al*. 2011). However, our results shed light on chloroplast functions linked to PD regulation. Firstly, we determined the molecular function of ISE2 in group II intron splicing in organelle. Moreover, we demonstrated that ISE2 is physically bound to organelle transcripts. Secondly, we identified a new *ise* mutant among the previously characterized chloroplasts mutants, *clpr2*. The gene Clpr2 encodes one of the subunits of the Clp protease system needed for plastidic ribosome assembly, protein degradation, recycling and translation (Kim *et al*. 2013). Interestingly, both *ise2* and *clpr2* exhibit altered splicing pattern for the four mRNAs assessed including *rpl2*, *clpP*, *atpF* and in minor degree with *rps12*. Interestingly, the splicing patterns of *clpP* between both mutants were different as can be observed in the Supporting Information Fig. S4. Enhanced band of approximately 1.5 kb is observed with intron-specific probe in *clpr2*. This band is also observed in the WT. Larger bands (>2 kb) are also visible in the mutant, indicating a certain degree of splicing defects in *clpr2*, which is consistent to results shown in Fig. 5a. The simple interpretation of these observations is that the splicing of the intron 1 type IIb splicing requires normal chloroplast protein homeostasis, and they are spliced less efficiently in *clpr2* (Kim *et al*. 2009; Asakura *et al*. 2012). In spite of this, *clpr2* is still able to process *clpP* mRNA (0.75 kb band in both WT and *clpr2*). In contrast, in *ise2* this putative mature mRNA 0.75 kb band is missing, indicating impaired splicing of both introns. In addition, we clearly detected the presence of larger bands (>2 kb) in *ise2*, which are hybridized with both exon and intron sequences, suggesting the more general splicing defects, and this is unlikely a consequence of potential translation impairment because MatK independent splicing also seems to be affected. Although, we cannot completely exclude an indirect effect because of translational defects of *ise2* on splicing regulation. Together with our RIP results indicating a direct interaction between ISE2 and *clpP* RNA, we concluded that ISE2 is a splicing factor.

Our results open the question whether chloroplast mutants with altered splicing may share similar PD defects. Nevertheless, we cannot discard the hypothesis that a direct signal from the chloroplast might control PD functions (Fig. 6). Several

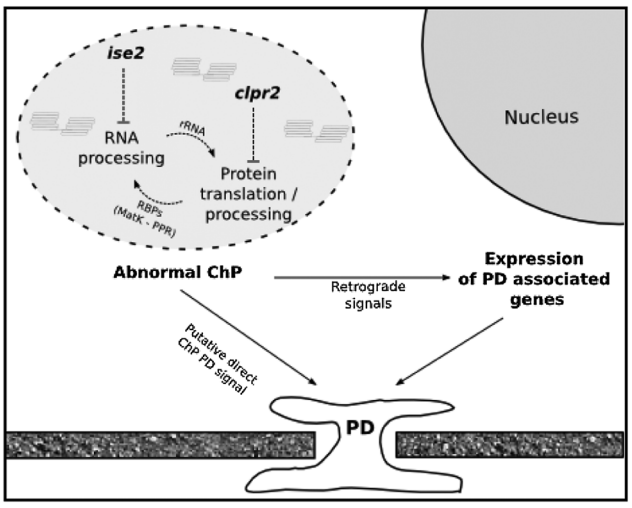

Figure 6. Model of chloroplast effect on plasmodesmata (PD) regulation. In *ise2* and *clpr2* mutants, defects of RNA splicing or the protein processing/translation results in an abnormal chloroplast development and a concomitantly PD deregulation (unregulated size exclusion limit), mediated either by retrograde signals that control putative PD-related nuclear genes, or by a putative plastid derived signal, or both.

chloroplasts compounds, including ROS and salicylic acid, can lead to callose production and deposition on PD (Wang *et al.* 2013). Our findings support the idea that chloroplast-dependent molecular mechanism impacts PD functions and modulates cell-to-cell communication in plants.

ACKNOWLEDGMENTS

We thank ABRC for providing the seeds. We thank Sara Maldonado for the epifluorescent microscope. We thank Micaela Godoy Herst and Franco Lencina for their help with primers and antibodies. We thank Fernando Bravo-Almonacid and Silvia Villamil for their support with Northern blots. We really appreciate and thank our colleagues Carolina Perez-Castro and Alejandra Attorresi for their invaluable helps with confocal microscopy and real-time PCR. This work was supported by CONICET and ANPCyT from Argentina, and The Saclay Plant Sciences Labex, Agence Nationale de la Recherche ANR-10-LABX-40 and an EMBO short-term fellowship to N. C.

REFERENCES

Asakura Y., Galarneau E., Watkins K.P., Barkan A. & van Wijk K.J. (2012) Chloroplast RH3 DEAD box RNA helicases in maize and *Arabidopsis* function in splicing of specific group II introns and affect chloroplast ribosome biogenesis. *Plant Physiology* **159**, 961–974.

Aubourg S., Kreis M. & Lecharny A. (1999) The DEAD box RNA helicase family in *Arabidopsis thaliana*. *Nucleic Acids Research* **27**, 628–636.

Babiychuk E., Vandepoele K., Wissing J., Garcia-Diaz M., De Rycke R., Akbari H., … Kushnir S. (2011) Plastid gene expression and plant development require a plastidic protein of the mitochondrial transcription termination factor family. *Proceedings of the National Academy of Sciences of the United States of America* **108**, 6674–6679.

Beale S.I. (2011) Chloroplast signaling: retrograde regulation revelations. *Current Biology* **21**, R391–R393.

Benitez-Alfonso Y., Cilia M., San Roman A., Thomas C., Maule A., Hearn S. & Jackson D. (2009) Control of *Arabidopsis* meristem development by thioredoxin-dependent regulation of intercellular transport. *Proceedings of the National Academy of Sciences of the United States of America* **106**, 3615–3620.

Benitez-Alfonso Y., Jackson D. & Maule A. (2011) Redox regulation of intercellular transport. *Protoplasma* **248**, 131–140.

Brunkard J.O., Runkel A.M. & Zambryski P.C. (2013) Plasmodesmata dynamics are coordinated by intracellular signaling pathways. *Current Opinion in Plant Biology* **16**, 614–620.

Burch-Smith T.M., Brunkard J.O., Choi Y.G. & Zambryski P.C. (2011) Organelle-nucleus cross-talk regulates plant intercellular communication via plasmodesmata. *Proceedings of the National Academy of Sciences of the United States of America* **108**, E1451–E1460.

Burch-Smith T.M. & Zambryski P.C. (2010) Loss of INCREASED SIZE EXCLUSION LIMIT (ISE)1 or ISE2 increases the formation of secondary plasmodesmata. *Current Biology* **20**, 989–993.

Burch-Smith T.M. & Zambryski P.C. (2012) Plasmodesmata paradigm shift: regulation from without versus within. *Annual Review of Plant Biology* **63**, 239–260.

Chi W., He B., Mao J., Li Q., Ma J., Ji D., … Zhang L. (2012) The function of RH22, a DEAD RNA helicase, in the biogenesis of the 50S ribosomal subunits of *Arabidopsis* chloroplasts. *Plant Physiology* **158**, 693–707.

Church G.M. & Gilbert W. (1984) Genomic sequencing. *Proceedings of the National Academy of Sciences of the United States of America* **81**, 1991–1995.

Hammani K. & Barkan A. (2014) An mTERF domain protein functions in group II intron splicing in maize chloroplasts. *Nucleic Acids Research* **42**, 5033–5042.

Hess W.R., Hoch B., Zeltz P., Hubschmann T., Kossel H. & Borner T. (1994) Inefficient rpl2 splicing in barley mutants with ribosome-deficient plastids. *Plant Cell* **6**, 1455–1465.

Jenkins B.D., Kulhanek D.J. & Barkan A. (1997) Nuclear mutations that block group II RNA splicing in maize chloroplasts reveal several intron classes with distinct requirements for splicing factors. *Plant Cell* **9**, 283–296.

Kim I., Hempel F.D., Sha K., Pfluger J. & Zambryski P.C. (2002) Identification of a developmental transition in plasmodesmatal function during embryogenesis in *Arabidopsis thaliana*. *Development* **129**, 1261–1272.

Kim J., Olinares P.D., Oh S.H., Ghisaura S., Poliakov A., Ponnala L. & van Wijk K.J. (2013) Modified Clp protease complex in the ClpP3 null mutant and consequences for chloroplast development and function in *Arabidopsis*. *Plant Physiology* **162**, 157–179.

Kim J., Rudella A., Ramirez Rodriguez V., Zybailov B., Olinares P.D. & van Wijk K.J. (2009) Subunits of the plastid ClpPR protease complex have differential contributions to embryogenesis, plastid biogenesis, and plant development in *Arabidopsis*. *Plant Cell* **21**, 1669–1692.

Kobayashi K., Otegui M.S., Krishnakumar S., Mindrinos M. & Zambryski P. (2007) INCREASED SIZE EXCLUSION LIMIT 2 encodes a putative DEVH box RNA helicase involved in plasmodesmata function during *Arabidopsis* embryogenesis. *Plant Cell* **19**, 1885–1897.

Kroeger T.S., Watkins K.P., Friso G., van Wijk K.J. & Barkan A. (2009) A plant-specific RNA-binding domain revealed through analysis of chloroplast group II intron splicing. *Proceedings of the National Academy of Sciences of the United States of America* **106**, 4537–4542.

Lange H., Sement F.M. & Gagliardi D. (2011) MTR4, a putative RNA helicase and exosome co-factor, is required for proper rRNA biogenesis and development in *Arabidopsis thaliana*. *Plant Journal* **68**, 51–63.

Lange H., Zuber H., Sement F.M., Chicher J., Kuhn L., Hammann P., … Gagliardi D. (2014) The RNA helicases AtMTR4 and HEN2 target specific subsets of nuclear transcripts for degradation by the nuclear exosome in *Arabidopsis* thaliana. *PLoS Genetics* **10**, e1004564.

Lee K.H., Park J., Williams D.S., Xiong Y., Hwang I. & Kang B.H. (2012) Defective chloroplast development inhibits maintenance of normal levels of abscisic acid in a mutant of the *Arabidopsis* RH3 DEAD-box protein during early post-germination growth. *Plant Journal* **73**, 720–732.

de Longevialle A.F., Hendrickson L., Taylor N.L., Delannoy E., Lurin C., Badger M., … Small I. (2008) The pentatricopeptide repeat gene *OTP51* with two LAGLIDADG motifs is required for the *cis*-splicing of plastid *ycf3* intron 2 in *Arabidopsis thaliana*. *Plant Journal* **56**, 157–168.

Majeran W., Friso G., Asakura Y., Qu X., Huang M., Ponnala L., … van Wijk K.J. (2012) Nucleoid-enriched proteomes in developing plastids and chloroplasts from maize leaves: a new conceptual framework for nucleoid functions. *Plant Physiology* **158**, 156–189.

Maule A.J., Benitez-Alfonso Y. & Faulkner C. (2011) Plasmodesmata – membrane tunnels with attitude. *Current Opinion in Plant Biology* **14**, 683–690.

Melonek J., Mulisch M., Schmitz-Linneweber C., Grabowski E., Hensel G. & Krupinska K. (2010) Whirly1 in chloroplasts associates with intron containing RNAs and rarely co-localizes with nucleoids. *Planta* **232**, 471–481.

Mingam A., Toffano-Nioche C., Brunaud V., Boudet N., Kreis M. & Lecharny A. (2004) DEAD-box RNA helicases in *Arabidopsis thaliana*: establishing a link between quantitative expression, gene structure and evolution of a family of genes. *Plant Biotechnology Journal* **2**, 401–415.

Nishimura K., Ashida H., Ogawa T. & Yokota A. (2010) A DEAD box protein is required for formation of a hidden break in *Arabidopsis* chloroplast 23S rRNA. *Plant Journal* **63**, 766–777.

Nishimura M., Graham D. & Akazawa T. (1976) Isolation of intact chloroplasts and other cell organelles from spinach leaf protoplasts. *Plant Physiology* **58**, 309–314.

Nott A., Jung H.S., Koussevitzky S. & Chory J. (2006) Plastid-to-nucleus retrograde signaling. *Annual Review of Plant Biology* **57**, 739–759.

Olinares P.D., Kim J. & van Wijk K.J. (2010) The Clp protease system; a central component of the chloroplast protease network. *Biochimica et Biophysica Acta* **1807**, 999–1011.

Petrillo E., Godoy Herz M.A., Fuchs A., Reifer D., Fuller J., Yanovsky M.J., … Kornblihtt A.R. (2014) A chloroplast retrograde signal regulates nuclear alternative splicing. *Science* **344**, 427–430.

Ruwe H., Kupsch C., Teubner M. & Schmitz-Linneweber C. (2011) The RNA-recognition motif in chloroplasts. *Journal of Plant Physiology* **168**, 1361–1371.

Salmon M.S. & Bayer E.M. (2014) Dissecting plasmodesmata molecular composition by mass spectrometry-based proteomics. *Frontiers in Plant Science* **3**, 307.

Schmittgen T.D. & Livak K.J. (2008) Analyzing real-time PCR data by the comparative C(T) method. *Nature Protocols* **3**, 1101–1108.

Schmitz-Linneweber C. & Small I. (2008) Pentatricopeptide repeat proteins: a socket set for organelle gene expression. *Trends in Plant Science* **13**, 663–670.

Sjogren L.L., Stanne T.M., Zheng B., Sutinen S. & Clarke A.K. (2006) Structural and functional insights into the chloroplast ATP-dependent Clp protease in *Arabidopsis*. *Plant Cell* **18**, 2635–2649.

Stern D.B., Goldschmidt-Clermont M. & Hanson M.R. (2010) Chloroplast RNA metabolism. *Annual Review of Plant Biology* **61**, 125–155.

Stonebloom S., Brunkard J.O., Cheung A.C., Jiang K., Feldman L. & Zambryski P. (2012) Redox states of plastids and mitochondria differentially regulate intercellular transport via plasmodesmata. *Plant Physiology* **158**, 190–199.

Stonebloom S., Burch-Smith T., Kim I., Meinke D., Mindrinos M. & Zambryski P. (2009) Loss of the plant DEAD-box protein ISE1 leads to defective mitochondria and increased cell-to-cell transport via plasmodesmata. *Proceedings of the National Academy of Sciences of the United States of America* **106**, 17229–17234.

Wang X., Sager R., Cui W., Zhang C., Lu H. & Lee J.Y. (2013) Salicylic acid regulates plasmodesmata closure during innate immune responses in *Arabidopsis*. *Plant Cell* **25**, 2315–2329.

Woodson J.D. & Chory J. (2008) Coordination of gene expression between organellar and nuclear genomes. *Nature Reviews Genetics* **9**, 383–395.

Xu R.R., Qi S.D., Lu L.T., Chen C.T., Wu C.A. & Zheng C.C. (2011) A DExD/H box RNA helicase is important for K+ deprivation responses and tolerance in *Arabidopsis thaliana*. *FEBS Journal* **278**, 2296–2306.

Zheng B., MacDonald T.M., Sutinen S., Hurry V. & Clarke A.K. (2006) A nuclear-encoded ClpP subunit of the chloroplast ATP-dependent Clp protease is essential for early development in *Arabidopsis thaliana*. *Planta* **224**, 1103–1115.

Zybailov B., Rutschow H., Friso G., Rudella A., Emanuelsson O., Sun Q. & van Wijk K.J. (2008) Sorting signals, N-terminal modifications and abundance of the chloroplast proteome. *PLoS One* **3**, e1994.

Received 29 December 2014; received in revised form 23 June 2015; accepted for publication 24 June 2015

SUPPORTING INFORMATION

Additional Supporting Information may be found in the online version of this article at the publisher's web-site:

Figure S1. Subcellular localization of ISE2-GFP. a) Western blot of ISE2-GFP leaf extracts revealed with anti-GFP.
Figure S2. Agarose denaturing gel image of RNA sample.
Figure S3. Drawing showing the primer positions.
Figure S4. Northern blot analysis Total RNA (3 µg) of WT, *ise*2 and *clpr*2 mutant plants were analyzed in denaturing agarose gels. Estimated sizes of bands are indicated. Probe identity is indicated for each blot.
Table S1. List of oligos sequences
Table S2. RIP control for DNA contaminants using *rpl*2 oligos